Sensors and Materials, Vol. 27, No. 10 (2015) 917–924
MYU Tokyo

S & M 1128

Thermoelectric Properties of SnO_2 Ceramics Codoped with Sb and Zn Prepared by Reactive Spark Plasma Synthesis Followed by Thermal Treatment

Shun-ichi Yanagiya*, Shu Furuyama, Itaru Uriya[1] and Masatoshi Takeda[1]

Department of Production Systems Engineering, National Institute of Technology, Hakodate College, 14-1 Tokura-cho, Hakodate, Hokkaido 042-8501, Japan
[1]Department of Mechanical Engineering, Nagaoka University of Technology, 1603-1 Kamitomioka-machi, Nagaoka, Niigata 940-2188, Japan

(Received February 13, 2015; accepted August 4, 2015)

Key words: thermoelectrics, oxide materials, reactive spark plasma synthesis, doping

The thermoelectric (TE) properties of SnO_2 codoped with Sb and Zn were investigated. Polycrystalline ceramics of n-type SnO_2-based semiconductors ($Sn_{1-2x}Sb_xZn_xO_2$, x = 0, 0.01, 0.03, 0.05, 0.07) were prepared by reactive spark plasma synthesis followed by thermal treatment at a temperature of 1123 K. X-ray diffraction (XRD) analysis showed that most of the XRD peaks could be assigned to peaks of the pure SnO_2 phase. The x = 0.05 and 0.07 samples showed the formation of a Zn_2SnO_4 secondary phase along with the main SnO_2 phase. Microstructural analysis by scanning electron microscopy showed that the average grain sizes of the Sb and Zn codoped samples were larger than that of the undoped sample. The highest TE power factor in this study was 1.20×10^{-4} $Wm^{-1}K^{-2}$, which was comparable to the previously reported value for the sample synthesized by conventional normal pressure sintering at 1573 K. The synthesis method we describe here is very effective for the low-temperature synthesis of SnO_2-based TE ceramics.

1. Introduction

Thermoelectric (TE) materials can directly convert heat to electricity; therefore, they are very important for thermal sensors and for harvesting waste heat such as that produced in power plants, garbage furnaces, and car engines. TE generators, however, have not been widely used to generate electricity because they are still inefficient and expensive. Thus, much effort has been expended, including in materials development, to improve the TE conversion efficiency. Various interesting TE materials have been reported to date such as tellurides,[1,2] silicon germanium,[3] silicides,[4,5] zinc

*Corresponding author: e-mail: yanagiya@hakodate-ct.ac.jp

ISSN 0914-4935

antimonides,[6] skutterudites,[7] clathrates,[8] half-Heusler alloys,[9] nanostructured materials,[10,11] and oxides.[12] This last group of materials has been extensively investigated after the discovery of the good TE properties of the layered cobalt oxide Na_xCoO_2[13] because of their high thermal and chemical stabilities at high temperatures in air.

TE materials are evaluated using the figure of merit, $ZT = TS^2\sigma/\kappa$, where T is the absolute temperature, S is the Seebeck coefficient, and σ and κ are the electrical and thermal conductivities, respectively. Although this equation shows that a large S, a high σ, and a small κ are required for a high ZT, these three parameters are interrelated, which makes achieving a high ZT difficult.

Tin oxide (SnO_2) is an interesting and attractive material. Several of its potential applications, such as its use as an electrode for dye-sensitized solar cells and electrochromic devices,[14,15] a catalyst in chemical reactions,[16] a varistor,[17] and a material for gas sensor,[18] were previously reported. SnO_2 is an n-type semiconductor with high electrical conductivity, so this material is also expected to be suitable for use in TE devices. We previously reported the TE properties of SnO_2 ceramics codoped with Sb and Zn, $Sn_{0.97-x}Sb_{0.03}Zn_xO_2$ (x = 0, 0.01, 0.03), where Sb was used as an n-type dopant to increase the number of free electrons and Zn was used as a sintering aid to fabricate high-density samples.[19] The samples were prepared by cold isotropic pressing (CIP) and normal pressure sintering at a temperature of 1573 K for 10 h. We found that the TE power factor of the x = 0.03 sample was improved by the simultaneous increases in electrical conductivity and Seebeck coefficient. The highest TE power factor of the x = 0.03 sample was approximately 2×10^{-4} $Wm^{-1}K^{-2}$ at 1060 K, and this value was 126% higher than that of the undoped sample.

Spark plasma sintering (SPS) utilizes a pulsed high DC current along with uniaxial pressure to consolidate powders. This process allows one to obtain high-quality dense ceramics at relatively low temperatures and in short sintering times, typically a few minutes.[20] The mechanism of SPS has been described in detail in several papers.[21–23] It has also been recognized that chemical reactions can be carried out in SPS. Reactive SPS includes the synthesis and densification of materials in a single step and thus offers faster processing times.[24]

In this study, reactive SPS was employed to synthesize SnO_2-based samples, $Sn_{1-2x}Sb_xZn_xO_2$ (x = 0, 0.01, 0.03, 0.05, 0.07). The samples were prepared by reactive SPS followed by thermal treatment at a temperature of 1123 K. The temperature dependences of the electrical conductivity and Seebeck coefficient of the samples were measured from about 330 to 1073 K. The maximum TE power factor of 1.2×10^{-4} $Wm^{-1}K^{-2}$ was obtained at 1060 K for the x = 0.05 sample. Reactive SPS with post-thermal treatment was effective for the low-temperature synthesis of SnO_2-based TE materials.

2. Experimental Methods

The starting materials were commercially available SnO_2 (99.9%, Sigma Aldrich), Sb_2O_3 (99.99%, Sigma Aldrich), and ZnO (99.99%, Sigma Aldrich) powders. The powders were mixed in appropriate molar ratios and ground well in a mortar. Then, the

powder was loaded in a cylindrical graphite die with an inner diameter of 15 mm. A carbon sheet of 0.2 mm thickness was inserted between the graphite die and the powder to avoid their reaction. The synthesis was carried out in vacuum using an SPS apparatus (SPS-511S, Sumitomo Coal Mining Company Ltd.). The powder mixture was heated from room temperature to 1123 K in 10 min and then held at that temperature for 10 min. A uniaxial pressure of 30 MPa in the die was applied during the entire process. The subsequent thermal treatment in air was carried out for all the samples at 1123 K for 24 h both to remove carbon from and to supply oxygen to the samples.

The constituent phases of the samples were determined by X-ray diffraction (XRD) using a Rigaku Ultima IV diffractometer, and intensity data were collected in the 2θ range of 20–70° with Cu-Kα radiation. The microstructure of the fracture surfaces of the samples was observed by a JEOL scanning electron microscope (SEM; JSM-6360LA). The electrical conductivity σ and Seebeck coefficient S were simultaneously measured using an ULVAC-ZEM2 system from about 330 to 1073 K under a partial helium pressure.

3. Results and Discussion

Figure 1 shows the XRD patterns of the $Sn_{1-2x}Sb_xZn_xO_2$ (x = 0, 0.01, 0.03, 0.05, 0.07) ceramics. All XRD peaks can be indexed to peaks of the SnO_2 rutile phase (ICCD card PDF #41-1445) except for the small amount of the secondary phase of Zn_2SnO_4 in the x = 0.05 and 0.07 samples. These results indicate that the samples doped up to x = 0.03 are single-phase. The solubility limit of Zn in the samples is less than 5 at.%.

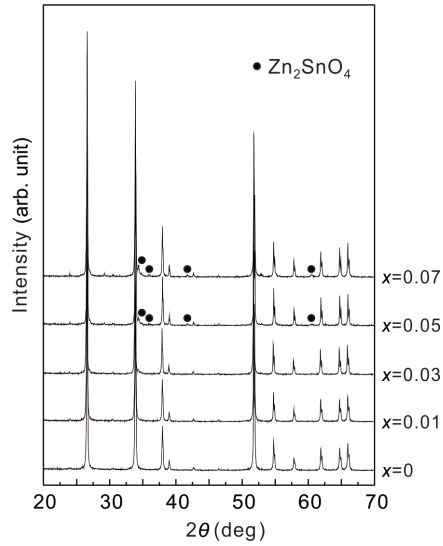

Fig. 1. XRD patterns of $Sn_{1-2x}Sb_xZn_xO_2$ (x = 0, 0.01, 0.03, 0.05, 0.07) ceramics.

Figure 2 shows the SEM micrographs of the fracture surfaces of the samples. The undoped (x = 0) sample consisted of agglomerated particles several sub-micrometers in size, which is smaller than that of previously reported samples prepared by CIP and normal pressure sintering.[19] The grain growth strongly depended on the doping concentration of Sb and Zn. The grain size increased as the amounts of Sb and Zn were increased up to x = 0.05, and then decreased with further increases in x. This result is in qualitative agreement with the results obtained by Saadeddin *et al*.[25] They reported that the bulk density of SnO_2 ceramics codoped with Sb and Zn (SnO_2:$Sb_{0.06}$:Zn_x) increased significantly as Zn^{2+} content increased from x = 0 to 0.06; then, the bulk density decreased with higher Zn values. The decrease in bulk density was considered to arise from the formation of the secondary phase of Zn_2SnO_4.

The temperature dependence of the electrical conductivity for the samples with different x values is shown in Fig. 3. The electrical conductivity of the undoped sample

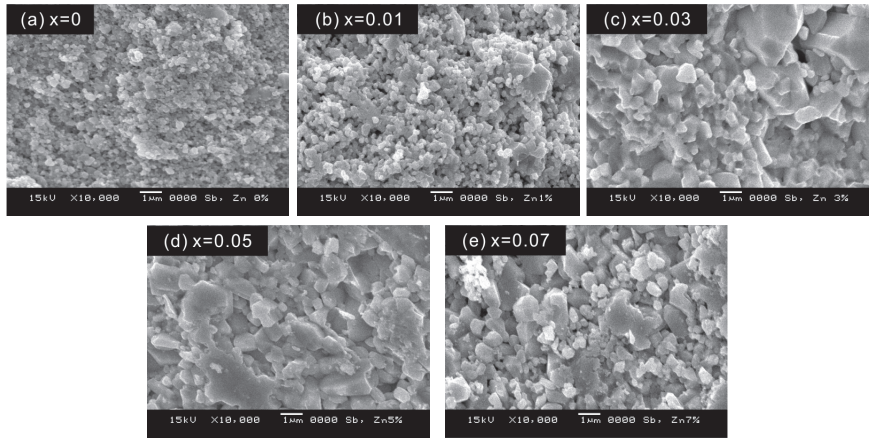

Fig. 2. SEM images of fracture surfaces of $Sn_{1-2x}Sb_xZn_xO_2$ ceramics: x = (a) 0, (b) 0.01, (c) 0.03, (d) 0.05, and (e) 0.07.

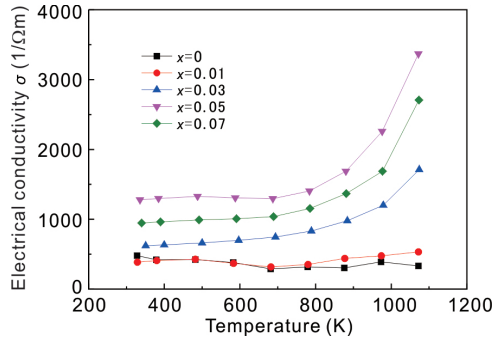

Fig. 3. (Color online) Temperature dependence of the electrical conductivity of $Sn_{1-2x}Sb_xZn_xO_2$ (x = 0, 0.01, 0.03, 0.05, and 0.07) ceramics.

showed a weak temperature dependence. This behavior with temperature is very similar to that observed for the undoped SnO_2 prepared by CIP and normal pressure sintering,[19] but the electrical conductivity of the sample in this study was about 1/3 that of the sample in ref. 19. The reason for the low electrical conductivity may be the smaller grain size, which reduces carrier mobility owing to scattering at grain boundaries. For the samples with x = 0.03, 0.05, and 0.07, the electrical conductivity increased monotonically with increasing temperature. The sample with x = 0.05 showed the highest electrical conductivity among the other samples over the entire temperature range, although the x = 0.07 sample had the highest doping concentration of Sb and Zn. The decrease in the electrical conductivity of the x = 0.07 sample compared with the x = 0.05 sample is probably due to both the decrease in grain size and the increase in the amount of the insulating inverse spinel phase of Zn_2SnO_4.[25] The highest value of 3.37×10^3 $\Omega^{-1}m^{-1}$ was obtained for the sample with x = 0.05 at 1072 K.

The temperature dependence of the Seebeck coefficients of the samples is shown in Fig. 4. The Seebeck coefficients of the samples are negative in the measured temperature range, indicating that the majority carriers are electrons. The absolute Seebeck coefficient $|S|$ for every sample increased continuously with increasing temperature over the entire temperature range. The temperature behavior of the samples can be classified into two groups: the first one comprises the undoped and x = 0.01 samples, and the second group comprises the x = 0.03, 0.05, and 0.07 samples. For general semiconductor materials, the Seebeck coefficient depends on carrier concentration; generally, the Seebeck coefficient decreases with increasing carrier concentration.[26] Therefore, this temperature behavior implies that the samples in the same group have similar quantities of charge carriers; for example, the carrier concentrations for the undoped and x = 0.01 samples are similar. The results for the second group show that the electron carrier concentrations of the three samples seem to saturate at x = 0.03. For the sample with x = 0.05, the highest absolute Seebeck coefficient of about 190 μV/K was obtained at 1072 K. This value is about twice as large as that of the sample showing the highest TE power

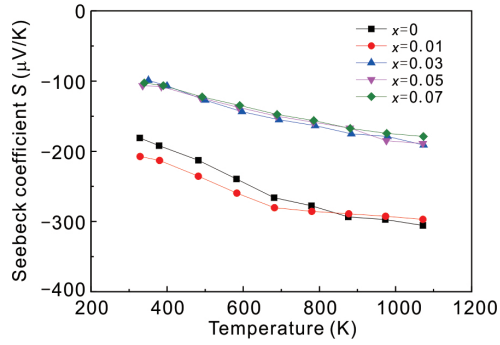

Fig. 4. (Color online) Seebeck coefficient as a function of temperature for $Sn_{1-2x}Sb_xZn_xO_2$ (x = 0, 0.01, 0.03, 0.05, and 0.07) ceramics.

factor (σS^2) in ref. 19. This suggests that the sample in this study has a lower carrier concentration than the sample in ref. 19. The low carrier concentration and smaller grain size of the sample in this study may be the reasons for the low electrical conductivity in this sample.

The temperature dependence of the calculated TE power factor is plotted in Fig. 5. The TE power factors of all the samples increased with increasing temperature. The $x = 0.05$ sample showed the highest TE power factor in the higher temperature region. This high TE power factor was primarily due to the increase in electrical conductivity compared with that in the other samples. The highest TE power factor of 1.20×10^{-4} $Wm^{-1}K^{-2}$ was obtained at 1072 K. This highest value is comparable to that of the sample prepared by CIP and normal pressure sintering at a temperature of 1573 K,[19] which is 450 K higher than the temperature in this study. Table 1 shows the sintering conditions and the values of TE parameters of the samples showing the highest power factors in this study and ref. 19. The reactive SPS method with post-thermal treatment was confirmed to be effective for synthesizing SnO_2-based TE ceramics at lower temperatures.

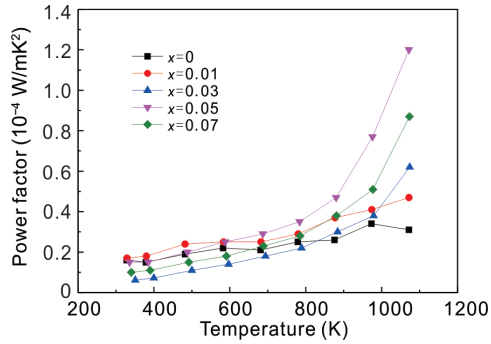

Fig. 5. (Color online) Temperature dependence of the TE power factor (σS^2) of $Sn_{1-2x}Sb_xZn_xO_2$ ($x = 0$, 0.01, 0.03, 0.05, and 0.07) ceramics.

Table 1
Comparison of the sintering conditions and TE parameters of the samples showing the highest power factors in this study and ref. 19.

	This study	Ref. 19
Preparation method	SPS	CIP
Sintering temperature (K)	1123	1573
Measuring temperature (K)	1072	1060
Electrical conductivity σ ($\Omega^{-1}m^{-1}$)	3.37×10^3	1.83×10^4
Seebeck coefficient S (μV/K)	−189	−108
Power factor σS^2 ($Wm^{-1}K^{-2}$)	1.20×10^{-4}	2.13

The ability to produce materials at low temperatures reduces production costs, leading to commercial advantage. We believe that a higher TE power factor can be achieved at a temperature of 1123 K, at which the samples were synthesized in this study, by adjusting the conditions. In particular, an increase in uniaxial pressure during reactive SPS will make samples more dense, increasing carrier mobility, electrical conductivity, and TE power factor.

4. Conclusions

We demonstrated a method of synthesizing SnO_2-based ceramics ($Sn_{1-2x}Sb_xZn_xO_2$, x = 0, 0.01, 0.03, 0.05, and 0.07) at a low temperature of 1123 K using reactive spark plasma synthesis followed by thermal treatment. XRD measurements showed that all the samples were single-phase with a rutile structure except the x = 0.05 and 0.07 samples, which had small amounts of the Zn_2SnO_4 secondary phase. The grain size strongly depended on the doping concentrations of Sb and Zn. The sample with x = 0.05 showed the largest average grain size and the highest electrical conductivity of 3.37×10^3 $\Omega^{-1}m^{-1}$ at 1072 K. The absolute Seebeck coefficient $|S|$ of every sample increased with increasing temperature. The results of the temperature dependence of the Seebeck coefficient imply that the carrier concentrations of the samples seem to saturate at x = 0.03. The TE power factor was maximized to a value of 1.20×10^{-4} $Wm^{-1}K^{-2}$ at 1073 K for the x = 0.05 sample. We confirmed that the method combining reactive SPS with post-thermal treatment was very effective for the low-temperature synthesis of SnO_2-based TE ceramics.

Acknowledgements

This work was supported by a research grant from Nagaoka University of Technology.

References

1 H. Scherrer and S. Scherrer: Thermoelectrics Handbook: Macro to Nano, ed. D. M. Rowe (CRC Press, Boca Raton, FL, USA, 2006) pp. 27-1–27-16.
2 K. Kurosaki, A. Kosuga, H. Muta, M. Uno and S. Yamanaka: Appl. Phys. Lett. **87** (2005) 061919-1.
3 S. Bathula, M. Jayasimhadri, N. Singh, A. K. Srivastava, J. Pulikkotil, A. Dhar and R. C. Budhani: Appl. Phys. Lett. **101** (2012) 213902-1.
4 M. Ito, T. Tada and S. Hara: J. Alloy Compd. **408**–**412** (2006) 363.
5 V. K. Zaitsev, M. I. Fedorov, E. A. Gurieva, I. S. Eremin, P. P. Konstantinov, A. Yu. Samunin and M. V. Vedernikov: Phys. Rev. B **74** (2006) 045207-1.
6 G. J. Snyder, M. Christensen, E. Nishibori, T. Caillat and B. B. Iversen: Nat. Mater. **3** (2004) 458.
7 H. Li, X. Tang, X. Su and Q. Zhang: Appl. Phys. Lett. **92** (2008) 202114-1.
8 S. Deng, Y. Saiga, K. Kajisa and T. Takabatake: J. Appl. Phys. **109** (2011) 103704-1.
9 S. R. Culp, S. J. Poon, N. Hickman, T. M. Tritt and J. Blumm: Appl. Phys. Lett. **88** (2006) 042106-1.

10 B. Poudel, Q. Hao, Y. Ma, Y. Lan, A. Minnich, B. Yu, X. Yan, D. Wang, A. Muto, D. Vashaee, X. Chen, J. Liu, M. S. Dresselhaus, G. Chen and Z. Ren: Science **320** (2008) 634.
11 A. J. Minnich , M. S. Dresselhaus, Z. F. Ren and G. Chen: Energy Environ. Sci. **2** (2009) 466.
12 J. He, Y. Liu and R. Funahashi: J. Mater. Res. **26** (2011) 1762.
13 I. Terasaki, Y. Sasago and K. Uchinokura: Phys. Rev. B **56** (1997) 12685.
14 S. Chappel and A. Zaban: Sol. Energy Mater. Sol. Cells **71** (2002) 141.
15 B. Orel, U. L. Štangar and K. Kalcher: J. Electrochem. Soc. **141** (1994) 127.
16 K. Sekizawa, H. Widjaja, S. Maeda, Y. Ozawa and K. Eguchi: Appl. Catal. A **200** (2000) 211.
17 P. R. Bueno, S. A. Pianaro, E. C. Pereira, L. O. S. Bulhões, E. Longo and J. A. Varela: J. Appl. Phys. **84** (1998) 3700.
18 E. R. Leite, I. T. Weber, E. Longo and J. A. Varela: Adv. Mater. **12** (2000) 965.
19 S. Yanagiya, N.V. Nong, J. Xu, M. Sonne and N. Pryds: J. Electron. Mater. **40** (2011) 674.
20 Z. A. Munir, U. Anselmi-Tamburini and M. Ohyanagi: J. Mater. Sci. **41** (2006) 763.
21 M. Omori: Mater. Sci. Eng. A **287** (2000) 183.
22 Z. Shen and M. Nygren: Chem. Rec. **5** (2005) 173.
23 R. Orru, R. Licheri, A. M. Locci, A. Cincotti and G. Cao: Mater. Sci. Eng. R **63**, (2009) 127.
24 A. M. Locci, R. Orrù and G. Cao: J. Mater. Res. **20** (2005) 734.
25 I. Saadeddin, H. S. Hilal, B. Pecquenard, J. Marcus, A. Mansouri, C. Labrugerea, M. A. Subramanian and G. Campet: Solid State Sci. **8** (2006) 7.
26 D. M. Rowe: Thermoelectrics Handbook: Macro to Nano, ed. D. M. Rowe (CRC Press, Boca Raton, FL, USA, 2006) pp. 1-1–1-14.